

# The binding site of bisphenol A to protein disulphide isomerase

Received August 2, 2011; accepted August 18, 2011; published online October 5, 2011

Shoko Hashimoto, Keiko Shimoto,  
Kazushi Okada\* and Susumu Imaoka†

Research Center for Environmental Bioscience, Department of Bioscience, School of Science and Technology, Kwansei Gakuin University, Sanda 669-1337, Japan

\*Department of Pharmacology, Toxicology and Therapeutics, University of Kansas Medical Center, 3901 Rainbow Boulevard, Kansas City, KS 66160, USA.

†Corresponding author: Susumu Imaoka, PhD, Department of Bioscience, School of Science and Technology, Kwansei Gakuin University, 2-1 Gakuen, Hyogo, Sanda 669-1337, Japan. Tel/Fax: +81-79-565-7673, email: imaoka@kwansei.ac.jp

**Protein disulphide isomerase (PDI) has been isolated as a binding protein of bisphenol A (BPA) in the rat brain. In this study, we determined binding sites of BPA to PDI and characterized the binding site. First, we identified the BPA-binding domain with ab, b'a'c, a, b, b' and a'c fragment peptides of PDI by surface plasmon resonance spectroscopy. BPA interacted with ab, b'a'c, a and b', suggesting that a and b' domains are important in their interaction. Second, ab, b'a'c, a,b,b'a', abb'a', abb', b'a', Δb' and a'c fragment peptides were used for their isomerase activity with RNase as a substrate. BPA could inhibit the activity of peptide fragments including b', suggesting that b' domain contributes to inhibition of catalytic activity of PDI by BPA. Next, we investigated the BPA-binding capacity of PDI by amino acid substitution. PDI lost the BPA-binding activity by the mutation of H258 and mutation of Q245 and N300 also decreased its activity. Furthermore, acidic condition increased the BPA-binding activity of PDI. These results suggest that the charge of these amino acid especially, H258, is important for the BPA to bind to PDI.**

**Keywords:** bisphenol A/circular dichroism spectra/fluorescence analysis/protein disulphide isomerase (PDI)/surface plasmon resonance.

**Abbreviations:** BPA, bisphenol A (2,2-bis(4-hydroxyphenyl)-propane); CD, circular dichroism; ERRγ, estrogen-related receptor gamma; E<sub>2</sub>, 17β-estradiol; HSQC, heteronuclear singlequantum correlation; NMR, nuclear magnetic resonance; PDI, protein disulphide isomerase; PDIp, pancreas-specific protein disulphide isomerase; RNase A, ribonuclease A; SPR, surface plasmon resonance; T<sub>3</sub>, 3,3',5-triiodo-L-thyronine.

Bisphenol A (BPA, 2,2'-bis(4-hydroxyphenyl) propane) is an endocrine-disrupting chemical that exhibits estrogen-like effects on animals (1). It has been

reported that prenatal and neonatal exposure to BPA in mice induces hyper-locomotion, decreases adaptability and enhances methamphetamine sensitization (2, 3). Recently, we found that exposure of *Xenopus* embryos to BPA induced malformation of the head region and a small-eye phenotype (4). These findings suggest that BPA exposure at an early developmental stage causes neuronal toxicity during embryonic development. In studying the mechanism of BPA effects on the central nervous system, a BPA-binding protein was isolated from the synaptosome fractions of the rat brain, and it was found to be protein disulphide isomerase (PDI) (5). PDI is a major protein in the lumen of the endoplasmic reticulum and a member of the thiorodoxin superfamily; it catalyses the formation, reduction or rearrangement of disulphide bonds of nascent or misfolded proteins or peptides (6, 7).

PDI is composed of **a**, **b**, **b'**, **a'** and **c** domains. The **a** and **a'** domains contain one catalytically active CGHC motif and thiol groups of cysteines involved in thiol-disulphide exchange (8). The **b** and **b'** domains are redox inactive. Crystal structure analysis of yeast PDI revealed that the protein is U-shaped, and the catalytic **a** and **a'** domains present on the same side of the protein (9). The surface of the inside of the U is a hydrophobic area that can interact with either unfolded or partially folded proteins containing exposed hydrophobic residues (9). The **b'** domain provides the principal peptide-binding site of PDI (10) and has an exposed hydrophobic patch that can interact with substrates (9). Cross-linking studies showed that the **b'** domain has a substrate-binding region that can interact with radiolabelled model peptides (10). Denisov *et al.* (11) performed an NMR analysis of the **bb'** domain of human PDI and found that the HSQC signal of many amino acid residues in the **bb'** domain is shifted by interaction of the **bb'** domain with substrates such as RNase, including T241, G251, H256, I318, T319 and E321. This result suggests that multiple amino acid residues are involved with the substrate binding. Also, there is a linker region between the **b'** and **a'** domains, which is called the **x**-linker (9, 11, 12). The **x**-linker is known to interact with the substrate-binding region of the **b'** domain, and substrates can compete with the **x**-linker in the **b'** domain. Therefore, the **x**-linker is considered to act as a gate for substrates to access to substrate-binding site and to modulate PDI activity (13).

PDI has other functions than as a thiol-disulphide catalyst. PDI is a binding protein of thyroid hormone (T<sub>3</sub>) or oestrogen (E<sub>2</sub>) (14, 15), although the physiological significance of T<sub>3</sub> binding to PDI is not clear. Primm and Gilbert (16) proposed that high-capacity, low-affinity hormone sites of PDI serve as hormone reservoirs to buffer the hormone concentration in the cells. Tsibris *et al.* (14) proposed that PDI has

a significant similar region in its amino acid sequence to that of oestrogen receptor. Recently, Fu *et al.* (17) reported that the human pancreas-specific PDI homologue (PDIp), which is one of the PDI family proteins highly expressed in pancreatic acinar cells (18, 19), is an intracellular E<sub>2</sub>-binding protein that can modulate oestrogen actions in mammalian cells (17, 20). The PDIp's E<sub>2</sub>-binding site is located in a hydrophobic pocket between the **b** and **b'** domain, and H278 is especially important in interaction of PDIp with E<sub>2</sub>. The hydrogen bond is formed between PDIp-H278 and the 3-hydroxyl group of E<sub>2</sub>, and is essential for the interaction (21).

Previously, we investigated the effect of BPA on PDI-mediated isomerase activity. We found that phenolic compounds, including nonylphenol, octylphenol or hydroxylated polychlorinated biphenyl (PCB), specifically bind to PDI and inhibit isomerase activity of PDI (22–24). These results suggest that BPA and these compounds bind to PDI via hydroxyl group(s) of the benzene ring(s). However, the BPA-binding site of PDI has not been clarified. Here, we identified the BPA-binding domain and required amino acid sequence of PDI for BPA binding. Moreover, in order to clarify the involvement of substrate recognition by **b'** domain and BPA binding, we focused on the x-linker, and investigated the effects of BPA on fluorescence of tryptophan in x-linker.

## Materials and Methods

### Chemicals

2,2-bis(4-hydroxyphenyl) propane (bisphenol A) was purchased from Wako Pure Chemical Industries, Ltd. (Osaka, Japan). BPA-amine derivative was synthesized as described previously (5). Ribonuclease A (RNaseA) type III from bovine pancreas were purchased from Sigma-Aldrich Corp. (St Louis, MO, USA). BPA and other chemicals were dissolved in ethanol at 100 mM to make stock solutions, which were stored at –80°C. Appropriate vehicle controls were performed in all experiments.

### Construction of rat PDI fragment peptides

In this study, we used rat PDI, because we first identified the rat PDI as a BPA-binding protein, although human PDI has similar characteristics. Rat PDI cDNA was cloned as described previously (5). PDI fragment peptides: **ab** (1–219th amino acid), **b'a'c** (220–509), **a** (1–119), **b** (120–219), **b'** (220–353), **a'** (354–465), **c** (466–509), **abb'** (1–353), **abb'a'** (1–465), **b'a'** (220–465), **a'c** (354–509), **Δb'** (1–219, 354–509), **b'x** (232–370) and **Δa'** (120–509) were constructed as follows. Polymerase chain reaction (PCR) of each fragment peptide was performed with the following primers using full-length PDI cDNA as a template. PCR was done with High-Fidelity DNA Polymerase: denaturation at 94°C for 2 min, and then 30 cycles of 94°C for 30 s, 55°C for 30 s and 72°C for 1 min. The primers used and the combinations of primers for PCR are shown in Supplementary Tables S1–S4. The **Δb'**, **b'x** mutants, full-length mutants and **Δa** mutants were constructed as follows. The **Δb'**, **b'x** mutants, full-length mutants and **Δa** mutants cDNAs were isolated in two steps by PCR. Nucleotide fragment 1 of **Δb'** was amplified with forward primer 1 and reverse primer 6. Nucleotide fragment 2 was amplified with forward primer 6 and reverse primer 5. The two amplified nucleotide fragments were purified by electrophoresis with agarose gels. The second round of PCR was performed with 2 nt fragments (nucleotide fragments 1 and 2) and two primers (forward primer 1 and reverse primer 5). Similarly, **b'x** mutants were constructed with 2 nt fragments. For example, in the case of I291A (I60 of **b'x**), nucleotide fragment 1 was amplified with forward primer 7 and reverse primer 8, and nucleotide fragment 2 was amplified with forward primer 8 and reverse primer 7. Then, second-round PCR was done with 2 nt

fragments and two primers (forward primer 7 and reverse primer 7). Other mutants, including L362A (L131 of **b'x**), H258A (H27), H258L, E244Q (E13), E244A, Q245E (Q14), Q245A, D299N (D68), D299A, N300D (N69), N300A Q245E/N300D, R302A (R71) of **b'x**, full-length mutants and **Δa** mutants were constructed in the same method. The amplified nucleotide fragments were subcloned into pGEM-T easy by the TA cloning method according to the manufacturer's instruction. The cDNA constructs **a**, **b**, **b'**, **ab**, **abb'**, **abb'a'**, **b'a'**, **Δa**, **Δb'**, **bb'**, **b'x**, **b'x** mutants, full-length mutants and **Δa** mutants were cut with BamHI and Sall, and the constructs **a'** and **a'c** were cut with SphI and Sall. These nucleotide fragments were ligated into a pQE-80L vector (Qiagen, Valencia, CA, USA).

### Expression and purification of histidine-tagged PDI mutants

Rosetta gami B (Novagen, Madison, WI, USA) *Escherichia coli* cells transformed with pQE-80 L-encoding histidine-tagged rat PDI and mutants were grown at 37°C in 2× yeast extract-tryptone-rich medium containing 0.1 mg/ml ampicillin, 0.034 mg/ml kanamycin, 0.02 mg/ml tetracycline and 0.015 mg/ml chloramphenicol. Protein expression was induced by adding 1.0 mM isopropylthio-β-D-galactoside. After additional cultivation for 8 h, *E. coli* cells were harvested and suspended in a lysis buffer (50 mM NaH<sub>2</sub>PO<sub>4</sub>, pH 7.5, containing 300 mM NaCl, 1.0 mg/ml lysozyme and 20 mM imidazole). *Escherichia coli* cells were sonicated, and centrifuged at 50,000 g for 30 min. The resulting supernatant was loaded onto a Ni-NTA agarose column (Qiagen), and the protein was eluted with lysis buffer containing 250 mM imidazole.

### Surface plasmon resonance analysis

BPA was immobilized on the CM5 sensor chip (GE Healthcare, Piscataway, NJ, USA) by amine coupling methods, according to the instruction manual. Briefly, the CM5 sensor chip was activated by the injection of 70 μl of *N*-hydroxysuccinimide (NHS) and an 1-ethyl-3-(3-dimethylaminopropyl)carbodiimide (EDC) mixture, creating a reactive ester on the surface and then 140 μl of 500 μM BPA-amine derivative (dissolved in 100 mM borate buffer, pH 9.0), which has a linker and amino group (5), was pulsed. The immobilized chip was masked by 70 μl of ethanolamine. Analyses were performed at 25°C with the BIAcore 2000 system (BIAcore, Uppsala, Sweden) using HBS-EP buffer [10 mM HEPES, pH 7.4, containing 150 mM NaCl, 3 mM EDTA and 0.005% (v/v) Tween-20]. Regeneration of the chip surface was achieved by running 5 μl of regeneration buffer (100 mM Tris-HCl containing 6 M Guanidine) through the flow cell at 10 μl/min. PDI and mutants (10, 20, 50 μM) were perfused over the immobilized BPA at a flow rate of 10 μl/min, and the resonance changes were recorded. The sensorgram of the control chip was subtracted from that of the immobilized BPA chip. Data were analysed by nonlinear curve fitting of the Langmuir binding isotherm (for fragment peptides and **b'x**) or Heterogeneous ligand Parallel reaction (for full length) with BIA evaluation software.

### Isomerase activity of PDI fragment peptides

Isomerase activity was assayed as described previously (5). Briefly, reduced and denatured RNase A (8 μM) was incubated with PDI (1 μM) in 100 mM sodium phosphate buffer, pH 7.5, containing 4.5 mM cytidine 2',3'-cyclic monophosphate (cCMP), 2 mM EDTA, 1 mM GSH, 0.2 mM GSSG and with or without 100 μM BPA at 25°C in a final volume of 0.2 ml. The reaction was started by adding reduced and denatured RNase A. Changes in absorbance at 296 nm were monitored with a spectrophotometer, the Multiskan Spectrum instrument (Thermo Labsystems, Boston, MA, USA).

### Fluorescence spectrometry

Intrinsic fluorescence spectra of PDI mutants were measured in 50 mM sodium phosphate buffer, pH 7.5, with a Perkin/Elmer LS50 Fluorescence Spectrometer (excitation at 280 nm, and emission at 300–400 nm at 25°C).

### Circular dichroism spectroscopy

Circular dichroism (CD) spectra of PDI and mutants were obtained with a Jasco J-600 Spectropolarimeter (Jasco Corp., Tokyo, Japan). Measurements were performed using 0.4–1.5 μM PDI or fragment peptides at 25°C as an average of 10 scans from 200 to 250 nm, using a cell with a path length of 1 cm, measured at a scan speed of

20 nm/min, a spectral bandwidth of 1.0 nm and a time constant of 2 s. The maximum voltage was below 1000 V.

## Results

### Identification of the BPA-binding domain in PDI

To identify the BPA-binding domain in PDI, we expressed histidine-tagged rat PDI fragment peptides in *E. coli* and purified them. Interaction between fragment peptides and BPA was investigated by Surface plasmon resonance (SPR) spectroscopy. PDI fragments (10, 20 and 50  $\mu\text{M}$ ) were perfused over the CM5 sensor chip immobilized BPA-amine derivative. Full-length PDI was confirmed to interact with BPA in a dose-dependent manner. Therefore, this assay system was found to be able to detect the binding of PDI to BPA. Accordingly, we initially determined whether the BPA-binding site is present in the N-terminus region (**ab**) or the C-terminus region (**b'a'c**). Both **ab** and **b'a'c** fragments interacted with BPA (Fig. 1). Furthermore, to determine which domains interact with BPA, we investigated the binding capability of each domain to

BPA, and calculated association rate constant ( $k_a$ ), dissociation rate constant ( $k_d$ ) and  $K_D$  values (Table I). We found that the **a** and **b'** domains bound to BPA in a dose-dependent manner, whereas the **b** and **a'c** domains did not bind to BPA at all. From  $K_D$  values, affinity of **b'** domain with BPA was much higher than that of **a** domain and this difference is due to their association rate constant  $k_a$ . These results suggest that PDI has two BPA-binding sites in the **a** and **b'** domains, especially **b'** domain is important domain for BPA binding.

### Isomerase activity of PDI fragment peptides

Previously, we found that BPA and  $T_3$  inhibit isomerase activity of PDI (5). To further explore the relationship between the inhibitory effect of BPA and BPA-binding efficiency, we examined the isomerase activity of fragment peptides in the presence of BPA. Eleven kinds of histidine-tagged fragment peptides (**ab**, **b'a'c**, **a**, **b**, **b'**, **a'**, **abb'a'**, **abb'**, **b'a'**,  $\Delta\text{b}'$  and **a'c**) were constructed and purified. First, to assess their

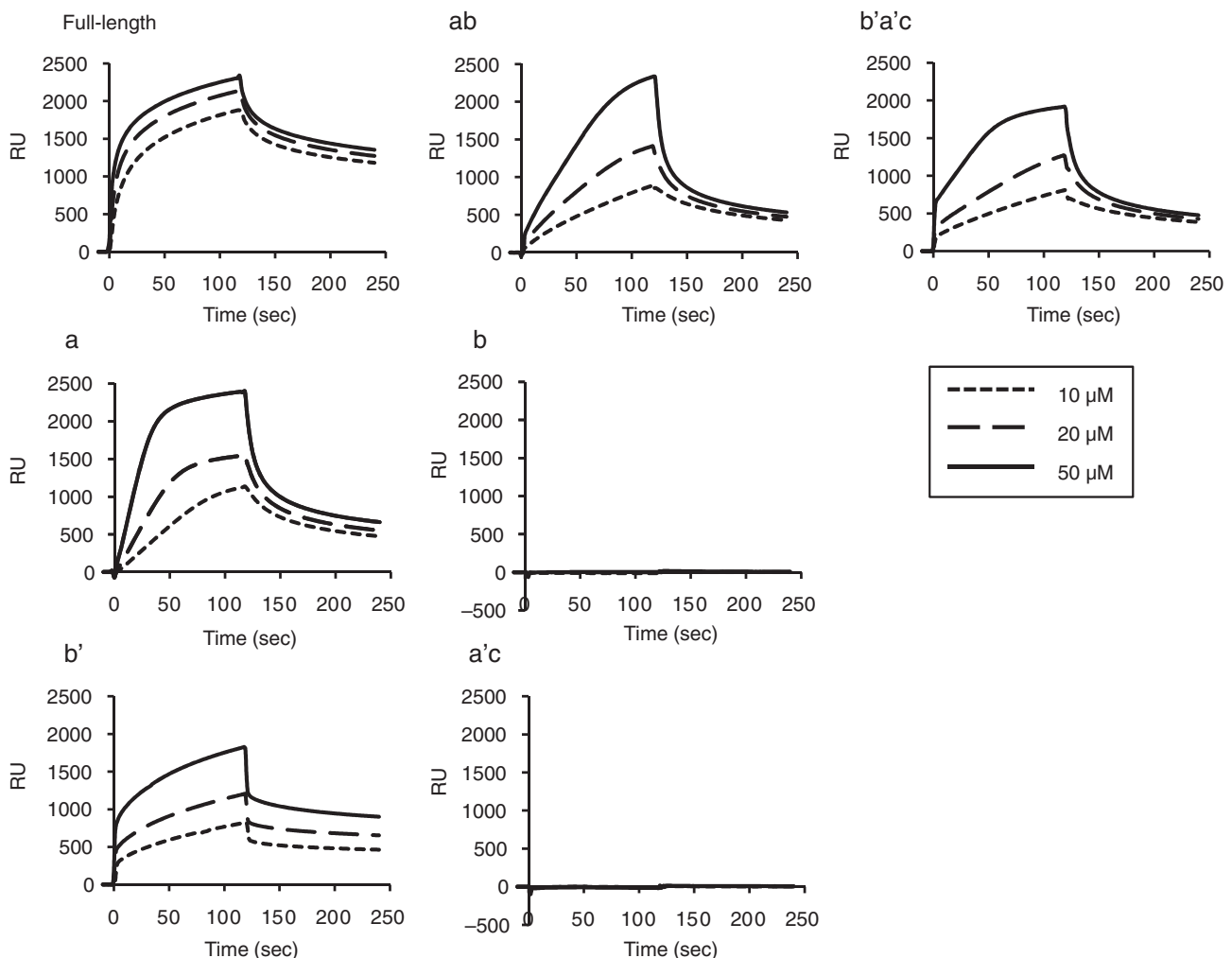


**Fig. 1** Interaction of BPA with PDI domains by SPR spectroscopy. BPA-amine derivative was immobilized on a sensor chip (CM5), and 10, 20 or 50  $\mu\text{M}$  of full-length PDI, **ab**, **b'a'c**, **a**, **b**, **b'** and **a'c** were pulsed at the cell flow rate of 10  $\mu\text{l}/\text{min}$ . Each sensor gram shows the resonance unit (RU) from which was subtracted the RU of the control sensor chip. The association of peptides with BPA was detected in 0–120 s, and dissociation was detected after 120 s. Data were analysed by nonlinear curve fitting of the Langmuir-binding isotherm with BIA evaluation software and are shown in Table I.



**Table I.** Association/dissociation rate constants and  $K_D$  values of each fragment peptide on BPA binding.

	$k_a$ (1/Ms)	$k_d$ (1/s)	$K_D$ (M)
ab	<100	$7.77 \times 10^{-3}$	$2.92 \times 10^{-3}$
b'a'c	$1.30 \times 10^2$	$5.27 \times 10^{-3}$	$4.04 \times 10^{-5}$
a	<100	$6.80 \times 10^{-3}$	$1.60 \times 10^{-4}$
b	ND	ND	ND
b'	$9.83 \times 10^2$	$1.36 \times 10^{-3}$	$1.39 \times 10^{-6}$
a'c	ND	ND	ND

Data in Fig. 1 were analysed by nonlinear curve fitting of the Langmuir-binding isotherm with BIA evaluation software ND, not detected.

folding, CD spectra of these fragments were measured (Supplementary Fig. S1). These fragment peptides maintained second structures,  $\alpha$ -helix and  $\beta$ -strand, suggesting that they have appropriate folding structures. Next, their isomerase activity was measured using RNase as a substrate. The full-length PDI (**abb'a'c**) and fragment peptides, **ab**, **b'a'c**, **abb'a'**, **abb'**,  **$\Delta$ b'** and **a'c**, had significant isomerase activity (Fig. 2A). Focusing on the inhibitory effect of isomerase activity by BPA, we note that the isomerase activity of fragment peptides containing the **b'** domain (full-length, **b'a'c**, **abb'a'** and **abb'**) was suppressed by BPA. On the other hand, the isomerase activity of fragment peptides that do not have the **b'** domain (**ab**, **a**,  **$\Delta$ b'** and **a'c**) were not affected by BPA, suggesting that BPA inhibits isomerase activity of PDI by binding to the **b'** domain. We also found that the inhibitory effects of  $T_3$  on isomerase activity of fragment peptides were similar to those of BPA (data not shown). Furthermore, we found that the isomerase activity of the **a'c** domain was enhanced by co-incubation with the **b'** domain but not the **b** domain (Fig. 2B). Enhancement of the isomerase activity by co-incubation with the **b'** domain was inhibited by BPA. These results strongly suggest that the **b'** domain is important in substrate binding to PDI and that binding of BPA to the **b'** domain inhibits the isomerase activity of PDI.

#### Interaction of the **b'** domain with the **a'c** domain

As described above, co-incubation of the **b'** domain, which does not include the **x**-linker, enhanced isomerase activity of the **a'c** domain, which includes the **x**-linker, and BPA inhibited the enhanced activity of the **a'c** domain by the addition of the **b'** domain. From these results, we predicted that the **b'** domain interacts with the **x**-linker included in the **a'c** domain. However, we could not detect direct interaction between the **a'c** and **b'** domains (data not shown). To assess the mechanism by which the **b'** domain enhanced the isomerase activity of the **a'c** domain, we examined the interaction between **a'c** and **b'** by fluorescence analysis (Fig. 3). By the crystal structure analysis of **b'x**, it was clarified that **x**-linker interacts with substrate-binding site of **b'** domain (12). In our study, **x**-linker is included in **a'c**, and **b'** does not have **x**-linker. Therefore, we predicted that **x**-linker of **a'c** interacts with **b'** domain, and this interaction may change the fluorescence of tryptophan

in **x**-linker. The **a'c** domain has three tryptophan residues (one of tryptophan exist in **x**-linker), but one tryptophan, which is near the isomerase active site in the **a'** domain, was shown to be heavily quenched by the active site (25), so we could detect the fluorescence of just two tryptophan residues. The **b'** domain, which does not contain an **x**-linker, has no tryptophan residue, and the **b** domain contains one tryptophan residue. First, **a'c** was mixed with **b** or **b'** and fluorescence was measured. The addition of **b** increased fluorescence intensity of **a'c** in a dose-dependent manner, because **b** itself has a tryptophan residue. On the other hand, co-incubation of the **b'** domain reduced the fluorescence intensity of **a'c**, suggesting that there is some interaction between **a'c** and **b'**. From these results, we considered that **x**-linker of **a'c** interacts with **b'**, and this interaction reduced the fluorescence of tryptophan in **x**-linker. Next, BPA was added to a mixture of **a'c** with **b'** or **b** and their fluorescence was measured. The addition of BPA did not change the fluorescence intensity of **a'c**, **b**, **b'** or a mixture of **a'c** and **b**, but it did recover the fluorescence intensity of a mixture of **a'c** and **b'**, indicating that BPA inhibits interaction between **b'** and **a'c**. These results suggest that the **b'** domain effectively interacts with the **a'c** domain and helps the folding or binding of substrates by the **a'c** domain, and BPA inhibits the interaction between **x**-linker of **a'c** and **b'**.

#### The effects of BPA on fluorescence of tryptophan in **x**-linker

Nguyen *et al.* (12) showed by fluorescence and NMR analysis that recombinant human PDI **b'x** can assume at least two different conformations in solution (12). One structure is the 'capping' form that the **x**-linker interacts with a substrate-binding site in the **b'** domain and the other is the 'uncapped' form of a substrate-binding site. They also found that human **b'x** mutant, I289A (I291A in rat PDI), showed a significant blue-shift in its fluorescence spectrum because the tryptophan residue of **x**-linker is in the hydrophobic environment compared with wild **b'x**, while L360A (L362A in rat PDI) showed red-shift. In other words, I289A forms in favour of the capping form, in which the **x**-linker caps the substrate-binding hydrophobic region of the **b'** domain. L362A forms in favour of the uncapped form and the tryptophan residue will be exposed to  $H_2O$ .

First, we constructed the I291A and L362A of the **b'x** domain of rat PDI, measured the fluorescence of tryptophan of the mutants, and confirmed that I291A showed a blue-shift and L362A showed a red-shift in the fluorescence spectrum compared with wild **b'x** (Fig. 4A). Next, we investigated the change of tryptophan fluorescence by BPA (Fig 4B). The fluorescence of wild **b'x** was decreased and maxima of fluorescence showed a red-shift in the presence of BPA with dose-dependent manner. Cumylphenol, which also binds to PDI and inhibits isomerase activity (22), changed the fluorescence spectrum in the same way as BPA, suggesting that BPA opens the **x**-linker of **b'x** and tryptophan of the **x**-linker is exposed to  $H_2O$ . On the other hand, diphenyl propane, which does not bind to PDI,

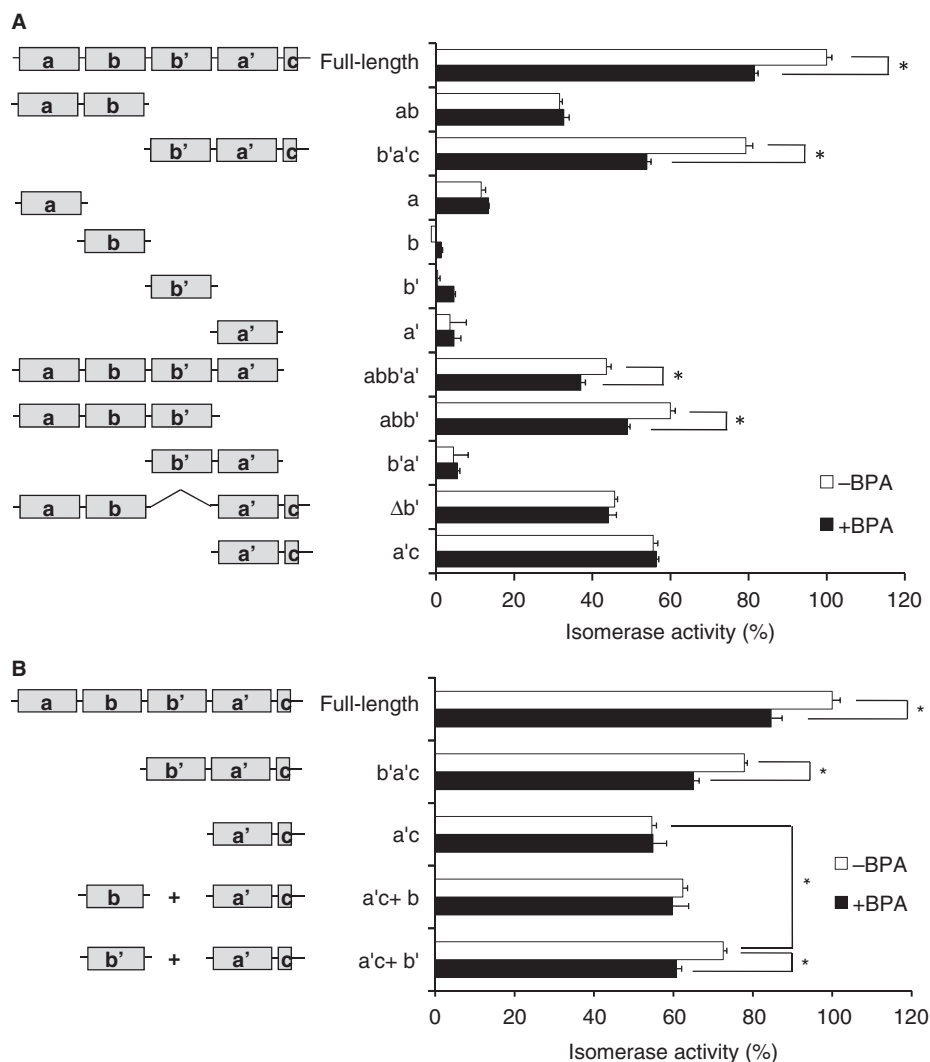


**Fig. 2 Isomerase activity of PDI fragment peptides.** (A) A refolding assay of reduced RNase A was performed using fragment peptides of PDI in the presence or absence of 100  $\mu$ M BPA. (B) Isomerase activities of a'c were measured in the presence of equal amounts of b or b' domain and 100  $\mu$ M BPA. The activity was calculated from the increase of absorbance at 296 nm/min. Isomerase activities were expressed as relative percentages when the value of isomerase activity of full-length PDI was set at 100%. Values are the mean  $\pm$  SD of three replicates, \* $P$  < 0.01 compared with the activity in the absence of BPA.

did not change the fluorescence spectrum. In the fluorescence spectrum of a'c, which includes the x-linker but does not bind to BPA, little reduction of fluorescence was observed in the presence of BPA, but fluorescence maximum was not shifted, suggesting the circumstance in tryptophan of x-linker of a'c was not changed by BPA. These results indicate that BPA binds to substrate binding site of b' domain and inhibit the interaction between x-linker and substrate binding site.

#### Effects of amino acid substitution in b'x on its binding to BPA

As the b'x domain appeared to be important in binding of BPA and in the inhibition of isomerase activity, the important amino acid residues in the b'x domain were identified. First, we assessed the BPA-binding activities of I291A and L362A by SPR analysis (Fig. 5A and Table II). I291A had lower association constant  $k_a$  with BPA than wild b'x. I291A is the capping form and access of BPA to b' domain may be difficult.

On the other hand, L362A b'x had higher  $k_d$  than wild b'x, suggesting that x-linker may be necessary for stabilization of substrate or ligand binding. Next, we searched critical amino acid residues in b'x to bind to BPA. Recently, Fu *et al.* (21) suggested that two amino acid residues, Q256 and H278, are important for PDIp to interact with  $E_2$  by the computer simulation analysis of the  $E_2$  and PDIp complex. Therefore, we chose the Q245 (corresponding to Q256 of PDIp) and H258 (corresponding to H278 of PDIp). Liu *et al.* (26) and Matsushima *et al.* (27) reported that oestrogen-related receptor gamma ( $ERR\gamma$ ) is a strong BPA-binding protein, and E275 or R316, and N346 in  $ERR\gamma$  interact with BPA by crystal structure analysis. Therefore, we chose glutamic acid, arginine, asparagine and aspartic acid residues from the core  $\beta$ -strand and  $\alpha$ -helices of b' domain that consist of the substrate binding region (13). Mutants of b'x, E244Q, E244A, Q245E, Q245A, H258A, H258L, D299N, D299A, N300D, N300A, R302A and

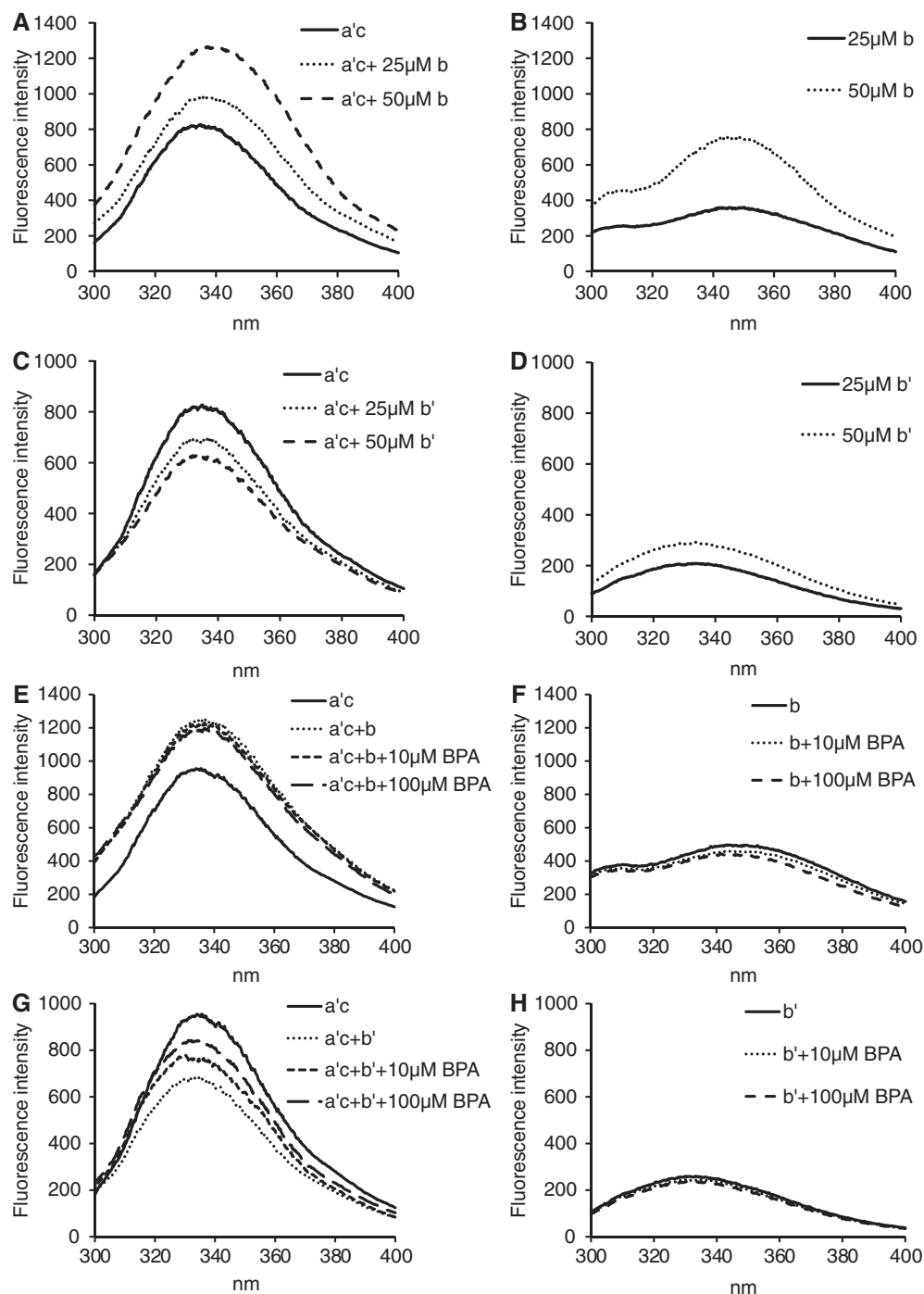


**Fig. 3** Fluorescence spectra of a'c, b and/or b' in the presence of BPA. Fluorescence spectra were measured in 20 mM sodium phosphate buffer, pH 7.5, at 25°C. The fluorescence emission was measured from 300 to 400 nm with excitation at 280 nm. (A) fluorescence spectrum of a'c (50 μM) in the presence or absence of b, (B) fluorescence spectrum of b, (C) fluorescence spectrum of a'c in the presence or absence of b', (D) fluorescence spectrum of b', (E) fluorescence spectrum of a'c in the presence or absence of b (50 μM) and/or BPA, (F) fluorescence spectrum of b in the presence or absence of BPA. (G) fluorescence spectrum of a'c in the presence or absence of b' (50 μM) and/or BPA and (H) fluorescence spectrum of b' in the presence or absence of BPA.

Q245E/N300D were prepared. The binding capabilities of these mutants purified from *E. coli* to BPA were assessed by SPR analysis. The E244Q, Q245A, D299N and N300A had almost similar  $k_a$  with wild b'x (Figs 5B–D and Table II). On the other hand, Q245E, N300D and R302A had lower  $k_a$  than wild b'x. H258L and H258A completely lost BPA-binding activity, suggesting H258 is the most important amino

acid residue in BPA binding. The double mutant, Q245E/N300D, were prepared and tested its BPA binding. As a result, Q245E/N300D also lost BPA-binding activity completely (Fig 5E). CD spectra of these mutants were measured to assess changes in the second structure of these proteins (Fig. 6). We found that the second structure of E244Q, Q245E, D299N, N300D and H258L were not changed, but H258A,

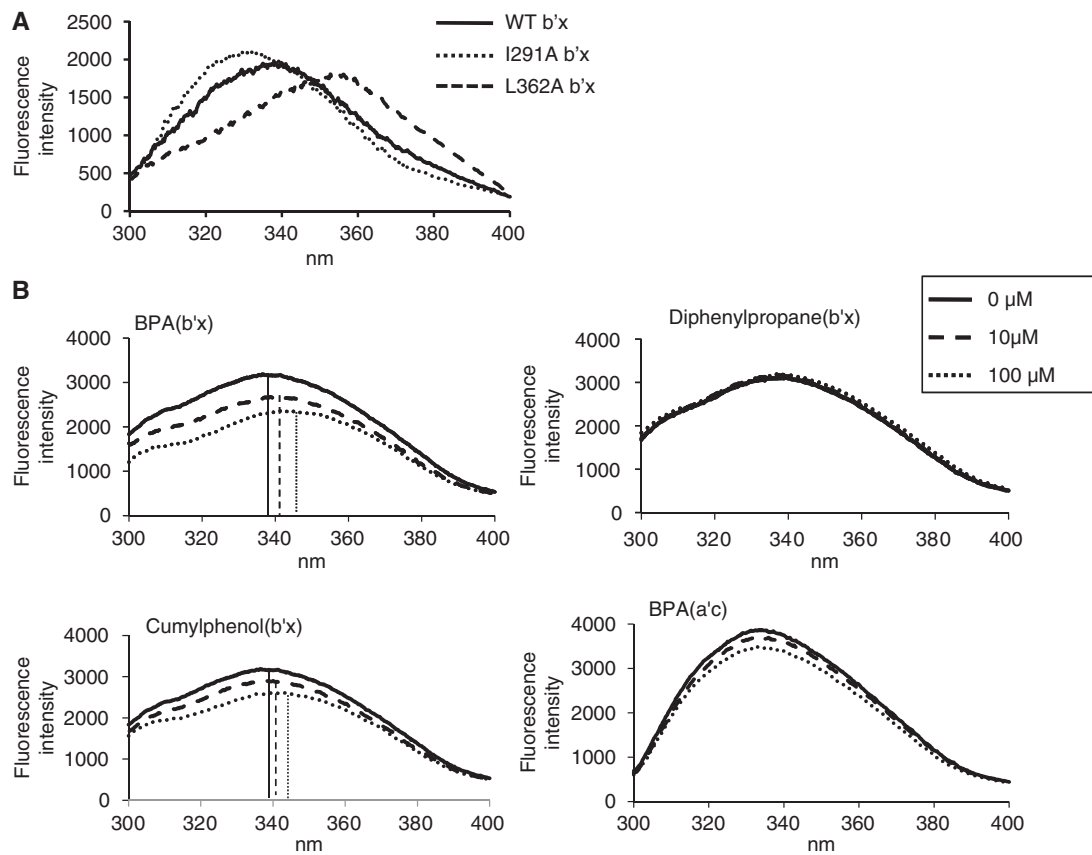


**Fig. 4** Fluorescence spectra of wild b'x, b'x mutants and a'c in the presence of BPA, cumylphenol or diphenylpropane. (A) Fluorescence spectra of wild b'x, I291A, and L362A. Fluorescence of wild b'x or mutants (100  $\mu$ M) was measured from 300 nm to 400 nm with excitation at 280 nm in 20 mM sodium phosphate buffer, pH7.5, at 25°C. (B) Fluorescence spectra of b'x (200  $\mu$ M) were measured in 20 mM sodium phosphate buffer, pH7.5, in the absence or presence of 10 or 100  $\mu$ M of BPA, cumylphenol or diphenylpropane at 25°C.

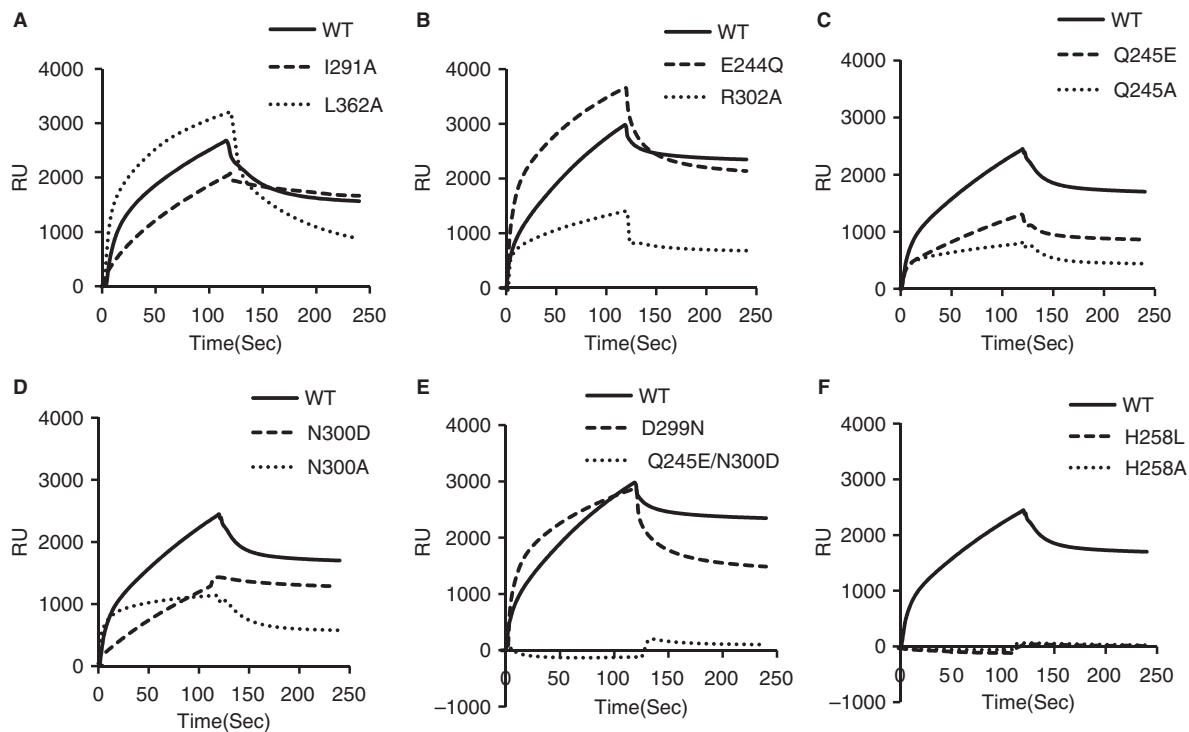


**Fig. 5** Binding of BPA to b'x mutants. BPA binding to b'x mutants was detected by SPR using a BPA-immobilized sensor chip. Each peptide (20  $\mu$ M) was pulsed for 120 s at a cell flow rate of 10  $\mu$ l/min. Data were analysed by nonlinear curve fitting of the Langmuir-binding isotherm with BIA evaluation software and are shown in Table II.

Q245E/N300D and R302A showed changes compared with wild **b'x**. In H258A, absorption around 209 nm was decreased, suggesting a decrease of  $\alpha$ -helix. In Q245E/N300D, absorption around 218 nm decreased, suggesting a decrease of  $\beta$ -strand. In R302A, both  $\alpha$ -helix and  $\beta$ -strand seemed to decrease. Other mutants appeared to maintain the second structures, as their CD spectra were not changed. Thus, reductions of BPA binding observed in Q245E, N300D and H258L were not due to the destruction of conformation by amino acid substitution. The amino acid

**Table II. Association/dissociation rate constants and  $K_D$  values of each fragment peptide on BPA binding.**

	$k_a$ (1/Ms)	$k_d$ (1/s)	$K_D$ (M)
WT	$1.40 \times 10^3$	$1.82 \times 10^{-3}$	$1.30 \times 10^{-6}$
I291A	$8.90 \times 10^2$	$1.13 \times 10^{-3}$	$1.27 \times 10^{-6}$
L362A	$1.92 \times 10^3$	$6.65 \times 10^{-3}$	$3.40 \times 10^{-6}$
E244Q	$1.70 \times 10^3$	$1.84 \times 10^{-3}$	$1.08 \times 10^{-6}$
Q245E	$7.36 \times 10^2$	$6.42 \times 10^{-4}$	$8.71 \times 10^{-7}$
Q245A	$1.50 \times 10^3$	$9.22 \times 10^{-3}$	$6.13 \times 10^{-6}$
D299N	$1.86 \times 10^3$	$3.05 \times 10^{-3}$	$1.64 \times 10^{-6}$
N300D	$2.34 \times 10^2$	$7.27 \times 10^{-4}$	$3.11 \times 10^{-6}$
N300A	$1.88 \times 10^3$	$2.51 \times 10^{-2}$	$1.34 \times 10^{-5}$
R302A	$9.34 \times 10^2$	$1.48 \times 10^{-3}$	$1.58 \times 10^{-6}$
H258L	ND	ND	ND
H258A	ND	ND	ND
Q245E/N300D	ND	ND	ND

Data in Fig. 5 were analysed by nonlinear curve fitting of the Langmuir-binding isotherm with BIA evaluation software. ND, not detected.

residues Q245, H258 and N300 may play an important role in BPA binding.

### Important amino acid residues to bind to BPA in full-length PDI

The Q245E/ N300D or H258L mutants of full-length PDI were constructed and purified. CD spectra of these mutants were measured (Supplementary Fig. S1). These mutants maintained second structures despite the amino acid substitutions. In case of **b'x**, double substitution of Q245 and N300 changed second structure. However, these substitutions of full-length PDI did not change the CD spectrum, suggesting that full-length PDI has more stable conformation than **b'x**. The full-length PDI mutants, Q245E/N300D and H258L, had lower BPA binding than wild-type PDI but they had significant BPA-binding activity (Fig.7A and Table III). Since the **a** domain can bind to BPA, **a** domain deletion mutants, Q245E/N300D  $\Delta a$  and H258L  $\Delta a$ , were prepared. H258L  $\Delta a$  completely lost BPA-binding activity but Q245E/N300D still had the activity, although its affinity with BPA was significantly decreased compared with wild PDI from  $K_D$  values (Fig.7B and Table IV). The amino acid residues, Q245, H258 and N300, which can form hydrogen bond with BPA, are critical for the BPA binding. Therefore, BPA binding of PDI was investigated under different pH conditions by SPR (Fig. 7C and Table V). The binding affinity of PDI to BPA increased in acidic condition. In acidic condition, polar amino acids in substrate-

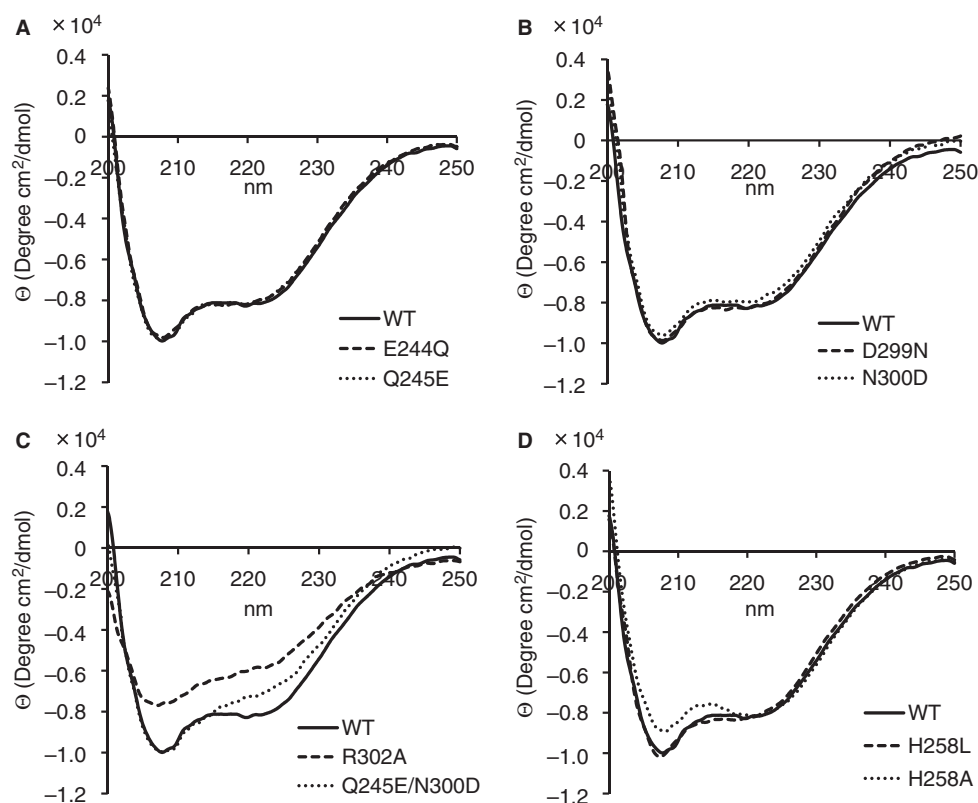


**Fig. 6 CD spectra of **b'x** mutants.** CD spectra of E244Q, Q245E (A), D299N, N300D (B), R302A, Q245E/N300D (C) and H258A, H258L (D) were measured from 200 to 250 nm. Measurements were performed using  $1.5 \mu\text{M}$  **b'x** at  $25^\circ\text{C}$ . Values (average of 10 scans) were converted to the mean molar ellipticity per residue ( $\theta$ ).



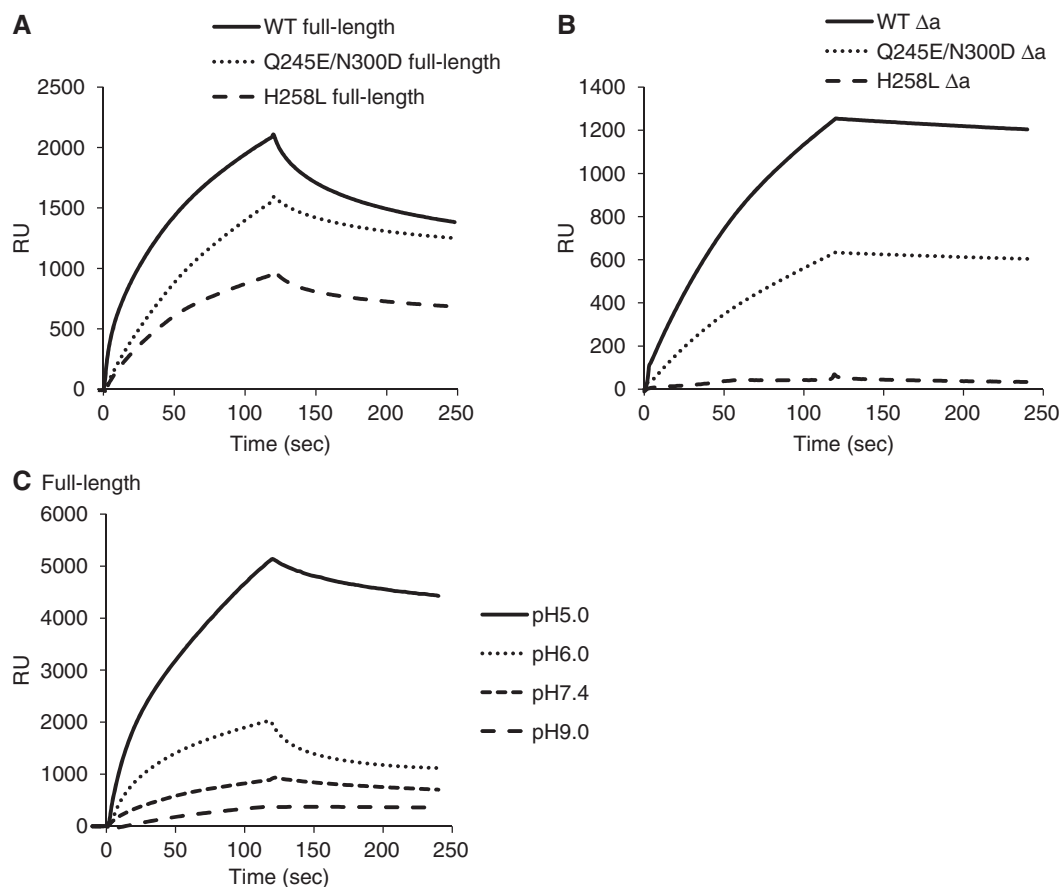


**Fig. 7 Binding of mutants of full-length PDI to BPA and effects of pH on binding of PDI to BPA.** (A and B) BPA binding to mutants of full-length PDI and to the **a** domain-deletion mutants ( $\Delta a$ ) were detected by SPR using a BPA-immobilized sensor chip. Each peptide (20  $\mu$ M) was pulsed for 120 s at a cell flow rate of 10  $\mu$ l/min. (C) Full-length PDI (10  $\mu$ M) in various pH of HBS-EP buffer [10 mM HEPES, containing 150 mM NaCl, 3 mM EDTA and 0.005% (v/v) Tween-20] were pulsed for 120 s at a cell flow rate of 10  $\mu$ l/min. Data were analysed by nonlinear curve fitting of the Langmuir-binding isotherm (for fragment peptides) or Heterogeneous ligand-parallel reaction (for full-length) with BIA evaluation software and are shown in Tables III–V.

**Table III. Association/dissociation rate constants and  $K_D$  values of full-length PDI mutants on BPA binding.**

	$k_a$ 1 (1/Ms)	$k_d$ 1 (1/s)	$K_D$ 1 (M)
WT full length	$3.08 \times 10^2$	$3.55 \times 10^{-6}$	$1.15 \times 10^{-8}$
Q245E/N300D full length	$2.21 \times 10^2$	$1.49 \times 10^{-4}$	$6.74 \times 10^{-7}$
H258L full length	$6.13 \times 10^2$	$3.13 \times 10^{-3}$	$5.10 \times 10^{-6}$

Data in Fig. 7A were analysed by nonlinear curve fitting of the Heterogeneous ligand-Parallel reaction with BIA evaluation software. In the analysis by Heterogeneous ligand Parallel reaction, two  $K_D$  values were obtained, but only higher affinity values ( $K_{D1}$ ) were shown.

binding region may be protonated and BPA is considered to access to its binding region easily as BPA is weak acid molecule. On the other hand, in basic condition, H258 is deprotonated. These results suggest that charges of amino acid residues in substrate (or ligand)-binding site are important for PDI to bind to BPA.

## Discussion

In this study, we found that PDI has two BPA-binding sites in the **a** and **b'** domains. Tsibris *et al.* (14)

**Table IV. Association/dissociation rate constants and  $K_D$  values of the **a** domain-deletion mutants ( $\Delta a$ ) on BPA binding.**

	$k_a$ (1/Ms)	$k_d$ (1/s)	$K_D$ (M)
WT $\Delta a$	$1.29 \times 10^3$	$1.79 \times 10^{-6}$	$1.39 \times 10^{-9}$
Q245E/N300D $\Delta a$	$8.79 \times 10^2$	$3.39 \times 10^{-4}$	$3.88 \times 10^{-7}$
H258L $\Delta a$	ND	ND	ND

Data in Fig. 7B were analysed by nonlinear curve fitting of the Langmuir-binding isotherm. ND, not detected.

proposed that PDI has a significant similar region with regard to amino acid sequence to that of oestrogen receptor. This sequence exists across the **a** and **b** domains, so we surmise that the binding site in the **a** domain is present in this sequence. Although the **b** domain did not show BPA binding in this study, the **b'** domain was newly identified as the ligand-binding domain. In fact, homology between **b** and **b'** domain is very low ( $\sim 18\%$ ) and **b** domain has no histidine residues, which has been identified as important amino acid residue in **b'** domain to bind to BPA. Furthermore, in the catalytic study with PDI fragment peptides, we found that full-length (**abb'a'c**), **ab**, **b'a'c**, **abb'a'**, **abb'**,  **$\Delta b'$**  and **a'c** had significant isomerase

**Table V. Association/dissociation rate constants and  $K_D$  values of full-length PDI on BPA binding under different pH conditions.**

	$k_{a1}$ (1/Ms)	$k_{d1}$ (1/s)	$K_{D1}$ (M)
pH 5.0	$1.01 \times 10^3$	$8.41 \times 10^{-7}$	$8.32 \times 10^{-10}$
pH 6.0	$2.80 \times 10^3$	$3.09 \times 10^{-6}$	$1.10 \times 10^{-9}$
pH 7.4	$1.48 \times 10^2$	$2.38 \times 10^{-6}$	$1.61 \times 10^{-8}$
pH 9.0	$1.53 \times 10^3$	$8.20 \times 10^{-4}$	$5.36 \times 10^{-7}$

Data in Fig. 7C were analysed by nonlinear curve fitting of the Heterogeneous ligand-Parallel reaction with BIA evaluation software. In the analysis by Heterogeneous ligand-Parallel reaction, two  $K_D$  values were obtained, but only higher affinity values ( $K_{D1}$ ) were shown.

activity, while **a**, **a'** and **b'a'** had a little or no isomerase activity, even though these fragments have isomerase active domains. These results suggest that the role of the **bb'** or **c** domain is important in isomerase activity. To confirm the importance of the **b'** domain in the inhibition by BPA, we investigated the isomerase activity of **a'c**, in the presence of the **b** or **b'** domain and BPA. Surprisingly, the isomerase activity of **a'c** was enhanced by co-incubation with the **b'** domain but not the **b** domain, and enhanced activity was inhibited by BPA. Several reports suggest that the **a'** domain can interact with the **b'** domain via flexible **x**-linker between **b'** and **a'** (9, 26). The **b'** domain involves in binding with substrates (10) and flexibility of **x**-linker (or **a'** domain) controls substrate binding to **b'** domain. From the fluorescence analysis of this study, BPA affects the interaction of **b'** and **a'c** containing **x**-linker. BPA may bind to this substrate-binding region competitively with **x**-linker or **a'** domain.

In order to clarify the effects of BPA on interaction between substrate-binding region of **b'** domain and **x**-linker, we tested the change of tryptophan fluorescence in **x**-linker of **b'x** by BPA. BPA induced the red-shift of the fluorescence peak of **b'x**, suggesting that BPA changed wild **b'x** to the uncapping form of **b'x**. In other words, BPA inhibited the interaction between **x**-linker and substrate recognition site of **b'** by binding to this site competitively with **x**-linker. Moreover, in SPR analysis with **b'x** mutants, capping (I291A) or uncapping (L362A) forms, the affinity of the capping form was lower than that of wild or uncapping **b'x**. This is because capping **x**-linker considered to prevent BPA to go into the BPA-binding site. Also, L362A **b'x** had a little higher dissociation rate and maximum of RU with BPA than wild **b'x**. One possible explanation is that L362A forms the uncapping form, and therefore access of BPA may be easy to interact **b'** domain. Another possible explanation is that the **x**-linker contributes to stabilization of substrate or ligand binding of PDI. Furthermore, in the gel filtration chromatography, WT and I291A **b'x** formed a monomer but L362A was present in mixture of monomer and dimer (data not shown). The L362A **b'x** tends to form a dimer due to its exposure of hydrophobic region. By the formation of dimer, apparently higher RU and dissociation rate may be detected in SPR analysis.

BPA is thought to bind to the **b'** domain via hydrogen bond with specific amino acids, because a hydroxyl group of the benzene ring of BPA is required (22, 24).

Therefore, we constructed several mutants by substitution of amino acid residues which have the potential to form hydrogen bonds. As a result, mutation of Q245 and N300 in full-length PDI reduced the BPA-binding activity and by the substitution of H258, PDI completely lost the BPA-binding activity, although these substitutions did not induce the drastic conformational changes by CD spectra. Furthermore, acidic condition increased BPA-binding activity of PDI. Thus, we suggest that the amino acid residues of H258 form hydrogen bonds with hydroxyl groups of BPA, and Q245 and N300 also involved in BPA binding.

PDIP also has binding activity to phenolic compounds such as  $E_2$ . PDI and PDIP have the highest homology of PDI family members. Klappa *et al.* (27) reported that PDIP requires the hydroxyl group for binding. The H258 of PDI corresponds to the H278 of PDIP. This histidine residue is suggested to be required for PDIP to bind to  $E_2$  (21). Here, we found some differences between PDI and PDIP with regard to chemical binding. First, PDI has two BPA-binding domains. Additionally, not only H258 but also some other amino acid residues are considered to be involved in the interaction with BPA. In fact, substitution of Q265 in PDIP, which corresponds to Q245 of PDI, did not affect the  $E_2$  binding (21). In the case of PDI, the **b'** domain alone is sufficient for BPA-binding activity, but the **b'** domain of PDIP alone does not exert  $E_2$ -binding activity. Ruddock *et al.* (28) suggested that the substrate recognition of PDI is also different from that of PDIP. The peptides containing tyrosine and tryptophan competed with radiolabelled somatostatin on PDIP, but these peptides cannot compete with somatostatin on PDI. At present, only PDI and PDIP are known to bind to small chemicals such as  $T_3$ ,  $E_2$  or BPA. These findings and our results indicate that the characteristics of PDI are somewhat different from those of PDIP in ligand binding, and these differentiations provide the distinct functions of these PDI proteins. However, to clarify the details of the ligand-binding functions, we need to conduct additional structural studies.

## Supplementary Data

Supplementary Data are available at *JB* online.

## Acknowledgements

We acknowledge Professor Shinichi Segawa (Kwansei Gakuin University) and Professor Hiroshi Yamaguchi (Kwansei Gakuin University) for their valuable discussions.

## Funding

Grant-in-Aid for Scientific Research from Japan Society for the Promotion of Science (B) (partial); Grant-in Aid from Hyogo Science and Technology Association (partial); Support Project to Assist Private Universities in Developing Bases for Research by the Ministry of Education, Culture, Sports, Science and Technology (partial); Grant-in-Aid from Kwansei Gakuin University (partial).

## Conflict of interest

None declared.

## References

- Obata, T. and Kubota, S. (2000) Formation of hydroxy radicals by environmental estrogen-like chemicals in rat striatum. *Neurosci. Lett.* **296**, 41–44
- Kawai, K., Nozaki, T., Nishikata, H., Aou, S., Takii, M., and Kubo, C. (2003) Aggressive behavior and serum testosterone concentration during the maturation process of male mice: the effects of fetal exposure to bisphenol A. *Environ. Health Perspect.* **111**, 175–178
- Suzuki, T., Mizuo, K., Nakazawa, H., Funae, Y., Fushiki, S., Fukushima, S., Shirai, T., and Narita, M. (2003) Prenatal and neonatal exposure to bisphenol-A enhances the central dopamine D1 receptor-mediated action in mice: enhancement of the methamphetamine-induced abuse state. *Neuroscience* **117**, 639–644
- Imaoka, S., Mori, T., and Kinoshita, T. (2007) Bisphenol A causes malformation of the head region in embryos of *Xenopus laevis* and decreases the expression of the ESR-1 gene mediated by Notch signaling. *Biol. Pharm. Bull.* **30**, 371–374
- Hiroi, T., Okada, K., Imaoka, S., Osada, M., and Funae, Y. (2006) Bisphenol A binds to protein disulfide isomerase and inhibits its enzymatic and hormone-binding activities. *Endocrinology* **147**, 2773–2780
- Ellgaard, L. and Ruddock, L.W. (2005) The human protein disulphide isomerase family: substrate interactions and functional properties. *EMBO Rep.* **6**, 28–32
- Maattanen, P., Kozlov, G., Gehring, K., and Thomas, D.Y. (2006) ERp57 and PDI: multifunctional protein disulfide isomerases with similar domain architectures but differing substrate-partner associations. *Biochem. Cell Biol.* **84**, 881–889
- Scherens, B., Dubois, E., and Messenguy, F. (1991) Determination of the sequence of the yeast YCL313 gene localized on chromosome III. Homology with the protein disulfide isomerase (PDI gene product) of other organisms. *Yeast* **7**, 185–193
- Tian, G., Xiang, S., Noiva, R., Lennarz, W.J., and Schindelin, H. (2006) The crystal structure of yeast protein disulfide isomerase suggests cooperativity between its active sites. *Cell* **124**, 61–73
- Klappa, P., Ruddock, L.W., Darby, N.J., and Freedman, R.B. (1998) The b' domain provides the principal peptide-binding site of protein disulfide isomerase but all domains contribute to binding of misfolded proteins. *EMBO J.* **17**, 927–935
- Denisov, A.Y., Maattanen, P., Dabrowski, C., Kozlov, G., Thomas, D.Y., and Gehring, K. (2009) Solution structure of the bb' domains of human protein disulfide isomerase. *FEBS J.* **276**, 1440–1449
- Nguyen, V.D., Wallis, K., Howard, M.J., Haapalainen, A.M., Salo, K.E., Saaranen, M.J., Sidhu, A., Wierenga, R.K., Freedman, R.B., Ruddock, L.W., and Williamson, R.A. (2008) Alternative conformations of the x region of human protein disulphide-isomerase modulate exposure of the substrate binding b' domain. *J. Mol. Biol.* **383**, 1144–1155
- Byrne, L.J., Sidhu, A., Wallis, A.K., Ruddock, L.W., Freedman, R.B., Howard, M.J., and Williamson, R.A. (2009) Mapping of the ligand-binding site on the b' domain of human PDI: interaction with peptide ligands and the x-linker region. *Biochem. J.* **423**, 209–217
- Tsibris, J.C., Hunt, L.T., Ballejo, G., Barker, W.C., Toney, L.J., and Spellacy, W.N. (1989) Selective inhibition of protein disulfide isomerase by estrogens. *J. Biol. Chem.* **264**, 13967–13970
- Obata, T., Kitagawa, S., Gong, Q.H., Pastan, I., and Cheng, S.Y. (1988) Thyroid hormone down-regulates p55, a thyroid hormone-binding protein that is homologous to protein disulfide isomerase and the beta-subunit of prolyl-4-hydroxylase. *J. Biol. Chem.* **263**, 782–785
- Primm, T.P. and Gilbert, H.F. (2001) Hormone binding by protein disulfide isomerase, a high capacity hormone reservoir of the endoplasmic reticulum. *J. Biol. Chem.* **276**, 281–286
- Fu, X.M. and Zhu, B.T. (2009) Human pancreas-specific protein disulfide isomerase homolog (PDIp) is an intracellular estrogen-binding protein that modulates estrogen levels and actions in target cells. *J. Steroid Biochem. Mol. Biol.* **115**, 20–29
- Desilva, M.G., Lu, J., Donadel, G., Modi, W.S., Xie, H., Notkins, A.L., and Lan, M.S. (1996) Characterization and chromosomal localization of a new protein disulfide isomerase, PDIp, highly expressed in human pancreas. *DNA Cell Biol.* **15**, 9–16
- Desilva, M.G., Notkins, A.L., and Lan, M.S. (1997) Molecular characterization of a pancreas-specific protein disulfide isomerase, PDIp. *DNA Cell Biol.* **16**, 269–274
- Fu, X.M., Dai, X., Ding, J., and Zhu, B.T. (2009) Pancreas-specific protein disulfide isomerase has a cell type-specific expression in various mouse tissues and is absent in human pancreatic adenocarcinoma cells: implications for its functions. *J. Mol. Histol.* **40**, 189–199
- Fu, X.M., Wang, P., and Zhu, B.T. (2011) Characterization of the estradiol-binding site structure of human pancreas-specific protein disulfide isomerase: indispensable role of the hydrogen bond between His278 and the estradiol 3-hydroxyl group. *Biochemistry* **50**, 106–115
- Hashimoto, S., Okada, K., and Imaoka, S. (2008) Interaction between bisphenol derivatives and protein disulphide isomerase (PDI) and inhibition of PDI functions: requirement of chemical structure for binding to PDI. *J. Biochem.* **144**, 335–342
- Okada, K., Hashimoto, S., Funae, Y., and Imaoka, S. (2009) Hydroxylated polychlorinated biphenyls (PCBs) interact with protein disulfide isomerase and inhibit its activity. *Chem. Res. Toxicol.* **22**, 899–904
- Okada, K., Hiroi, T., Imaoka, S., and Funae, Y. (2005) Inhibitory effects of environmental chemicals on protein disulfide isomerase in vitro. *Osaka City Med. J.* **51**, 51–63
- Lappi, A.K., Lensink, M.F., Alanen, H.I., Salo, K.E., Lobell, M., Juffer, A.H., and Ruddock, L.W. (2004) A conserved arginine plays a role in the catalytic cycle of the protein disulphide isomerases. *J. Mol. Biol.* **335**, 283–295
- Wang, C., Chen, S., Wang, X., Wang, L., Wallis, A.K., Freedman, R.B., and Wang, C.C. (2010) Plasticity of human protein disulfide isomerase: evidence for mobility around the X-linker region and its functional significance. *J. Biol. Chem.* **285**, 26788–26797
- Klappa, P., Freedman, R.B., Langenbuch, M., Lan, M.S., Robinson, G.K., and Ruddock, L.W. (2001) The pancreas-specific protein disulphide-isomerase PDIp interacts with a hydroxyaryl group in ligands. *Biochem. J.* **354**, 553–559
- Ruddock, L.W., Freedman, R.B., and Klappa, P. (2000) Specificity in substrate binding by protein folding catalysts: tyrosine and tryptophan residues are the recognition motifs for the binding of peptides to the pancreas-specific protein disulfide isomerase PDIp. *Protein Sci.* **9**, 758–764